This is a pre-print version of the paper. Please cite the final version of the paper:

G. Di Martino, A. Iodice, D. Riccio, and G. Ruello, “Equivalent Number of Scatterers for SAR Speckle Modeling,” *IEEE Trans. Geosci. Remote Sens.*, vol. 52, no. 5, pp. 2555-2564, May 2014. DOI: 10.1109/TGRS.2013.2262770.

Equivalent Number of Scatterers for SAR Speckle Modeling

Gerardo Di Martino, *Member, IEEE*, Antonio Iodice, *Senior Member, IEEE*,
Daniele Riccio, *Senior Member, IEEE*, Giuseppe Ruello, *Member, IEEE*

***Abstract* — In this paper the equivalent number of scatterers of a rough scattering surface is defined, physically justified, and evaluated.**

New generation space-borne SAR sensors are acquiring images at such a high ground resolution that quite often the statistics of these images do not match with those predicted by the classical Rayleigh speckle model. Non-Rayleigh speckle is frequently mathematically modeled via a K-distribution in terms of a parameter that presently can be estimated (i.e., *a-posteriori*) on the SAR images and is linked to the number of scatterers per resolution cell. However, to model and predict (i.e., *a-priori*) the statistical behavior of the SAR images, a full characterization of the scatterers is required. To this aim, the concept of equivalent number of scatterers of a rough scattering surface is here defined and physically justified. This parameter is then analytically evaluated in closed form as a function of the roughness of the illuminated surface and of SAR sensor parameters. The presented analytical evaluation applies to both classical and fractal descriptions of the surface roughness. Finally, the dependence of the equivalent number of scatterers on the roughness of the illuminated surface and on SAR sensor parameters is analyzed for a range of values of roughness parameters actually encountered in natural surfaces, and by considering typical system parameters of modern high-resolution space-borne SAR systems. It is shown that, actually, for some combinations of realistic surface and system parameters, the equivalent number of scatterers can be of the order of unity.

***Index Terms*— Synthetic Aperture Radar, Speckle, Rough Surfaces, Electromagnetic Scattering, Fractals.**

I. Introduction

SYNTHETIC Aperture Radar (SAR) images exhibit the well-known speckle phenomenon, due to fact that usually the signal backscattered by a SAR resolution cell is the coherent sum of random radar returns. When a natural, randomly rough, distributed surface is observed, this happens because SAR image resolution cell dimensions are much larger than the wavelength, λ, of the incident electromagnetic field. Due to the lack of deterministic knowledge about the structure of the surface at wavelength scale, a statistical description of the speckle phenomenon is usually adopted. The return from each resolution cell in the SAR image is

This work was supported by the EU-FP7 project "Development of Pre-Operational Services for Highly Innovative Maritime Surveillance Capabilities" (DOLPHIN).

The authors are with the Dipartimento di Ingegneria Elettrica e delle Tecnologie dell'Informazione, Università di Napoli Federico II, 80125, Napoli, Italy (e-mail: gerardo.dimartino@unina.it; iodice@unina.it; daniele.riccio@unina.it; ruello@unina.it).

modeled as the coherent sum of the returns coming from independent discrete scatterers randomly distributed within the resolution cell. Evidently, for a rough distributed surface the concept of "independent scatterers" has no direct physical meaning, and the idea itself of discrete scatterers sounds unreasonable; notwithstanding, this very simple mathematical model easily leads to interesting results, briefly recalled in the following, and therefore we think it is worth trying to relate it to the geometrical properties of the scattering surface.

The speckle model can be formalized as a random walk in the complex plane [1]-[4], where the key parameter for its statistical characterization is the number of independent scatterers per resolution cell, N. Under the hypothesis that $N>>1$, the central limit theorem can be applied giving rise to a circular complex Gaussian field, with Rayleigh distributed amplitude, and uniformly distributed phase. In this case the speckle is defined as *fully developed*. For low resolution SAR sensors, whose resolution cell area is of the order of tens of square meters (very large compared to the centimeter wavelength), the above mentioned hypothesis can be safely assumed and the Rayleigh amplitude model (or, equivalently, the Exponential intensity model) well matches actual data for almost every surface roughness. This model is very attractive because only the knowledge of the mean square value of the cell return is required for the speckle description, regardless of an detailed characterization of the scatterers. However, for modern space-borne very high resolution SAR sensors, the hypothesis of a resolution cell size much larger than the wavelength cannot be safely assumed, and the statistics of SAR images can depart from those predicted by the Rayleigh model. In particular, for sensors like Cosmo-SkyMed and TerraSAR-X the size of the resolution cell (in spotlight mode) is less than 1 m^2 against a wavelength of 3.1 cm; moreover, for forthcoming sensors which will operate in C (e.g., Sentinel-1), S (e.g., NovaSAR-S) and L (e.g., ALOS-2) bands (i.e., with wavelengths of the order of tens of centimeters) with resolutions of the order of few meters, the Rayleigh model will probably be even less accurate.

The K-distribution has been valuably used to model the statistical behavior of SAR images as a function of the number of scatterers per resolution cell for any N [4]. This distribution was originally introduced for its ability in modeling SAR image statistics of actual oceanic scenes for not large values of N. Moreover, the coherent sum of a finite number of (independent) random returns has been proved to be in general K-distributed [4]-[7]. Hence, non-Rayleigh statistics [4] and small number of scatterers per resolution cell were (on phenomenological bases) employed to deduce the occurrence of a significant degree of correlation between the scatterers in the resolution cell. However, especially in this case, a comprehensive physical and statistical characterization of the scatterers is required in order to adequately describe the speckle phenomenon. The concept of independent scatterers needs to be elucidated.

In this paper the concept of equivalent number of scatterers of a rough scattering surface is defined, physically justified and related to the surface roughness, based on a physical description of the scattering phenomenon within the resolution cell. Although the model can be also employed for sea surfaces, it applies to natural rough solid surfaces, such as bare or little

vegetated soils. At the best of our knowledge, very few papers in the open literature are focused explicitly on the characterization of speckle as related to the physical properties of this kind of surfaces [5], [7]. However, also in these works no practical definition of the concept of scatterer in presence of a distributed target is provided. For the first time, in the following a relation between the number of independent scatterers per resolution cell and the physical properties of the surface (roughness) and of the sensor (wavelength, look angle, resolution) is provided. The roughness of the illuminated surface is modeled either as a classical stationary Gaussian process or as a fractional Brownian motion (fBm) process [1], [8]-[11]. The phase contributions of the returns coming from each point in the resolution cell are evaluated: the difference in these phase terms characterizes the speckle present on the image.

The paper is organized as follows. Section II is devoted to summarize the basic concepts of the classical Exponential and K-distributed speckle models. In Section III we present the surface models employed to describe the resolution cell roughness. Section IV is devoted to introduce the electromagnetic approach that allows us evaluating the number of equivalent scatterers per resolution cell as a function of surface and sensor parameters. Finally, some concluding remarks are presented in Section V.

II. Speckle Mathematical Models

Most of the models available in literature describe the return from a resolution cell as the coherent sum of N electromagnetic returns [1]-[7]:

$$E = Ve^{j\phi} = \sum_{i=1}^{N} V_i e^{j\phi_i}, \qquad (1)$$

where $V_i e^{j\phi_i}$ is the contribution due to the i-th scatterer. Hence, the field E is a function of the number N of scatterers per resolution cell and, according to this value, the speckle will be Exponentially or K-distributed, as detailed in the following sub-sections.

A. Exponentially-distributed speckle

In the hypothesis that the number N of independent scatterers per resolution cell is very large, the central limit theorem can be used to evaluate the phase and amplitude of the field in terms of their pdfs [1]-[2]. In this case, the speckle is defined as fully developed and E turns out to be a circular complex Gaussian field, whose amplitude, intensity and phase are described by a Rayleigh, an exponential and a uniform distribution in $[0,2\pi]$, respectively.

Note that in this case only the knowledge of the mean square value of the cell return is required for the speckle description, regardless of a detailed characterization of the scatterers.

B. *K-distributed speckle*

If the hypothesis of a large number of independent scatterers per resolution cell does not hold, the problem of studying the coherent sum of a finite number of fields must be tackled. To obtain a closed form pdf for the return intensity, the following assumptions are made [4]: 1) the amplitudes V_i and the phases ϕ_i are statistically independent from each other and from V_j and ϕ_j if $i \neq j$; 2) the V_i are K-distributed; 3) the ϕ_i are uniformly distributed in [0,2π]. Under these hypotheses, the return intensity $w=|E|^2$ presents a pdf that can be expressed as [4]:

$$p_N(w) = \frac{b/\sqrt{w}}{\Gamma(M)}\left(\frac{b\sqrt{w}}{2}\right)^M \mathrm{K}_{M-1}\left(b\sqrt{w}\right), \qquad (2)$$

where the parameter M is related to the number of scatterers per resolution cell through the relation $M = N(1+\nu)$, b and ν are parameters depending on the mean of w[1], $\mathrm{K}_{M\text{-}1}(\bullet)$ is the second kind modified Bessel function of order M-1 and $\Gamma(\bullet)$ is the Euler Gamma function.

It can be shown that for M>>1, the distribution (2) reduces to a negative exponential function, which is in accordance with the Exponential model [4].

Note that the above described models are purely mathematical ones: they are certainly formally sound, but do not provide any physical-based reliable definition of the scatterers, and do not make any attempt to directly relate the number of scatterers to the physical parameters characterizing the observed surface (actually, they cannot). Leaving aside this preliminary definition, the idea itself of discrete (elemental) scatterers may sound unphysical for rough distributed surfaces; and the overall radar return, as a simple mathematical sum of elemental scattering values, appears formally too far from the typical behavior of any electromagnetic scattering approach valid for rough surfaces [1], [2], [9], [12].

III. Surface Description

The choice of an adequate model for the observed surface is crucial for scattering evaluation purposes. In the literature, widespread models describe the rough surface shape as a stationary Gaussian process [1], [2], [12]-[14]. However, in the last decades it was demonstrated that fractal models are the most reliable ones for the description of natural surfaces [8]-[11], [13]-[16]. In particular, only fractal models are able to take into account the scaling properties typical of natural surfaces [13]-[21].

In the following of this section both models are detailed. More details regarding the comparison of the classical and fractal models and the range of typical values of the roughness parameters of actual natural surfaces are reported in the Appendix.

[1] In particular, the value of b can be set in order to obtain the proper value of the mean of w. For further details on typical values of ν see [4].

A. Classical model

Classical models used for the description of random rough surfaces involve the definition of a pdf for the height of the surface. Usually, a zero-mean, σ^2 variance Gaussian distribution is used:

$$\Pr\{z < \bar{\zeta}\} = \frac{1}{\sqrt{2\pi}\sigma} \int_{-\infty}^{\bar{\zeta}} \exp\left(-\frac{\zeta^2}{2\sigma^2}\right) d\zeta, \quad (3)$$

where Pr{•} stands for "probability".

For scattering evaluation purposes also the second order statistical characterization is necessary. It is assumed that the stochastic process describing the surface is stationary (or, at least, wide sense stationary) and isotropic, so that its second order characterization can be provided through the normalized auto-correlation function $C(\tau) \triangleq \langle |z(x,y)z(x',y')|^2 \rangle / \sigma^2$, where τ is the distance between the points (x,y) and (x',y') and <•> stands for the statistical mean. In particular, the most widely used (single-scale) auto-correlation functions are the Gaussian and the Exponential ones [1], [2], [9], [13]-[21]. In the former case, we have:

$$C(\tau) = e^{-\frac{\tau^2}{L^2}}, \quad (4)$$

while in the latter:

$$C(\tau) = e^{-\frac{\tau}{L}}, \quad (5)$$

where L is the correlation length of the surface. More in general, in some cases intermediate Gaussian-Exponential models can be used [19]. They present autocorrelation functions of the following type:

$$C(\tau) = e^{-\left(\frac{\tau}{L}\right)^n}, \quad (6)$$

with $n \in [1,2]$; for n=1 and n=2 they reduce to the cases of (5) and (4), respectively.

Alternatively, the structure function $Q(\tau)$, i.e., the surface increments variance, can be used:

$$Q(\tau) \triangleq \langle |z(x,y) - z(x',y')|^2 \rangle = 2\sigma^2\big(1 - C(\tau)\big), \quad (7)$$

which, using (6), becomes

$$Q(\tau) = 2\sigma^2\left(1 - e^{-\left(\frac{\tau}{L}\right)^n}\right). \quad (8)$$

A stationary behavior for the height statistical process must be assumed to use σ and L as surface roughness descriptors: however, this hypothesis presents well-known problems in modeling the roughness of natural surfaces [11], [13]-[17]. An unambiguous definition of σ and L is not straightforward, thus complicating the deployment of effective measurement procedures. As a matter of fact, strict requirements must be fulfilled to obtain reliable measures of these parameters [13]-[15], [19], [21]. For this reason, in the following sub-section we introduce a powerful alternative fractal-based model for the quantitative description of the roughness of natural surfaces.

B. Fractal model

The above described conventional surface models are deficient for characterizing surface roughness because they do not take into account the statistical scale-invariance properties typical of natural surfaces [13]-[17]. Usually, fractal surface models are based on the fBm model [9], [22], [23]. The fBm is a non-stationary, everywhere continuous, nowhere differentiable process, described in terms of the pdf of its increments. A stochastic process $z(x,y)$ is an fBm surface if, for every x, x', y, y' it satisfies the following relation:

$$\Pr\{z(x,y) - z(x',y') < \bar{\xi}\} = \frac{1}{\sqrt{2\pi}T^{1-H}\tau^H}\int_{-\infty}^{\bar{\xi}} \exp\left(-\frac{\xi^2}{2T^{2-2H}\tau^{2H}}\right) d\xi, \quad (9)$$

where, as in the previous case, τ is the distance between the points (x,y) and (x',y') and the two parameters that control the fBm behavior are:

- H: the *Hurst coefficient* ($0<H<1$), related to the fractal dimension D by means of the relationship $D=3-H$.
- T [m]: the *topothesy*, i.e. the distance over which chords joining points on the surface have a surface-slope mean-square deviation equal to unity.

Using these two parameters we are able to completely describe the structure function of the surface, without any arbitrary choice of the autocorrelation function of the surface. In the fractal case the shape of the structure function derives directly from the incremental process characterization (9). In particular, the fBm structure function is by definition

$$Q(\tau) \triangleq \langle |z(x,y) - z(x',y')|^2 \rangle = T^{2-2H}\tau^{2H}. \qquad (10)$$

Note that both in the classical (8) and fractal (10) cases the structure function is an increasing function of the distance τ.

Finally, we explicitly note that no straightforward relation between the fractal parameters and the classical ones is available. As a matter of fact, the definition of "equivalent" σ and L involves the introduction of some kind of dependence on the observation scales of interest, thus providing quantities which are dependent on the size of the profile [9] and which for very large values of the profile length do not converge to the values of σ and L predicted by the classical models [9], [14], [15], [24].

IV. Electromagnetic Model

The SAR image is the superposition integral of the reflectivity function $\gamma(\bullet)$, weighted by the overall (i.e., including the focusing operation) SAR unit response $g(\bullet)$ [2], [25]:

$$i(x_0, y_0) = \iint \gamma(x,y) g(x_0 - x, y_0 - y) dxdy. \qquad (11)$$

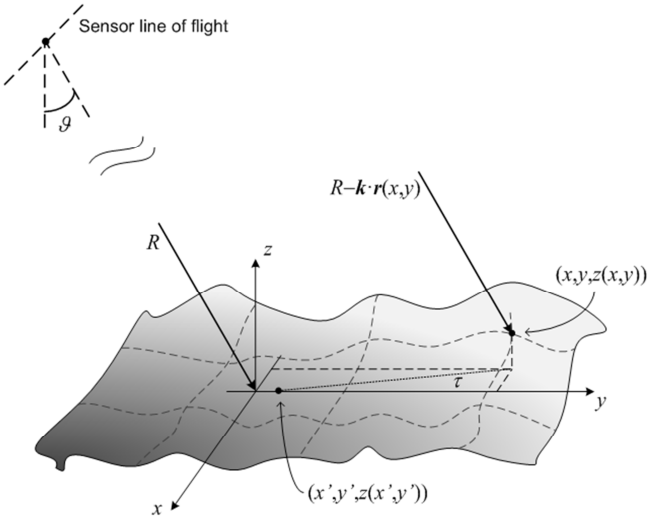

Fig. 1: Geometry of the scattering problem.

The function $g(\bullet)$ is assumed to be negligible outside an area A centered around (x_0,y_0), here defined as the "resolution cell". The reflectivity function $\gamma(x,y)$ can be expressed as the product of a factor S, which depends on the surface electric permittivity, the incidence angle and polarizations, and a (two-way) propagation factor $e^{-j2kR}e^{j2\boldsymbol{k}\cdot\boldsymbol{r}}$, which accounts for the phase contributions coming from the points of the resolution cell located in position $\boldsymbol{r} = x\hat{x} + y\hat{y} + z(x,y)\hat{z}$ [25]. Here, $\boldsymbol{k} = k_x\hat{x} + k_y\hat{y} + k_z\hat{z}$ is the electromagnetic propagation vector, so that $\|\boldsymbol{k}\| = k = 2\pi/\lambda$ [m^{-1}] [1], and R is the distance of the sensor from the origin of the reference system. If we reasonably assume that S is constant within a resolution cell, then (11) can be rewritten as

$$i(x_0,y_0) = Se^{-j2kR}\iint e^{j2\boldsymbol{k}\cdot\boldsymbol{r}(x,y)}g(x_0-x,y_0-y)dxdy = Se^{-j2kR}\iint e^{j2k_xx}e^{j2k_yy}e^{j2k_zz(x,y)}g(x_0-x,y_0-y)dxdy \quad (12)$$

where the randomness of $i(\bullet)$ is due to the presence of $z(x,y)$ in the phase term.

In order to still employ the simplified model (1), we can subdivide the resolution cell into smaller domains in such a way that electromagnetic returns pertaining to areas included into a single domain are strongly correlated, whereas returns from different domains are uncorrelated. The return from the whole resolution cell is then evaluated as the sum of returns from these domains. Within this framework each domain can represent (actually is the physical counterpart of) a single "scatterer", and, by definition, originates a radar return uncorrelated from those pertinent to the adjacent scatterers. Then, the equivalent number of scatterers per resolution cell is introduced as the ratio between the resolution cell area, A, and the equivalent scatterer area. Accordingly, it is important to choose a reliable rationale to define the equivalent scatterer size: one might be tempted to choose as scatterer (linear) size the roughness correlation length L. However, this choice is not suitable for the fractal case, in which no unique correlation length can be defined [9]-[11], [13], [14]; moreover, in the following, we show that this choice is in general wrong even in the classical case, although the surface correlation length turns out to be an upper bound for the (equivalent) scatterer size.

Geometry of the scattering problem is reported in Fig. 1, where ϑ is the sensor look angle and τ is the distance between two generic points located inside the resolution cell in positions (x',y') and (x,y), respectively.

To obtain a proper physical evaluation of the scatterer size, we define the scatterer radius τ_M as the distance between the two generic surface points (x,y) and (x',y'), such that the correlation between electromagnetic returns from the two points, i.e.

$$\langle e^{j2k_zz(x,y)}e^{-j2k_zz(x',y')}\rangle = \langle e^{-j2k_z(z(x',y')-z(x,y))}\rangle = e^{-\frac{(2k_z)^2}{2}Q(\tau)}, \quad (13)$$

TABLE I
SAR SENSOR PARAMETERS

Parameter	Value
Look angle, ϑ [deg]	30
Wavelength, λ [m]	$3.1 \cdot 10^{-2}$
Resolution cell area, A [m^2]	1

falls below a given threshold, say e^{-t}, with t of the order of unity. Accordingly the required value of τ_M must satisfy the following relation:

$$Q(\tau_M) = \frac{t}{2k_z^2}. \quad (14)$$

The above condition is fully compliant with the intrinsic hypothesis in (1) prescribing independency at the radar returns level, not at the surface level. In addition, condition (14) holds the remarkable property of being applicable to both classical and fractal models. Mathematically, (14) is equivalent to require that the standard deviation $2k_z\sqrt{Q(\tau_M)}$ of the phase difference between the contributions coming from points (x,y) and (x',y') is equal to $\sqrt{2t}$.

According to the previous definition, the correlation between the return from any point of the scatterer and the return from the scatterer center is greater than e^{-t}, or, equivalently, the phase difference between the return from any point of the scatterer and the return from the scatterer center has a standard deviation smaller than $\sqrt{2t}$.

In order to proceed with the explicit calculation of τ_M we now need to take into account the specific surface model. In the following the cases of classical and fractal surface models are separately investigated.

A. *Classical surface model*

In the classical case we can compute τ_M by using the definition of the structure function (7) into (14):

$$C(\tau_M) = 1 - \frac{t}{4k_z^2\sigma^2}. \quad (15)$$

Assuming the auto-correlation function in (6) we obtain:

$$\frac{\tau_M}{L} = \left[-\ln\left(1 - \frac{t}{4k_z^2\sigma^2}\right)\right]^{\frac{1}{n}}, \quad (16)$$

with $n \in [1,2]$.

For very rough surfaces presenting $4k_z^2\sigma^2 \gg t$ (with *t* of the order of unity), we can write:

$$\left(\frac{\tau_M}{L}\right)^n \cong \frac{t}{4k_z^2\sigma^2} \quad (17)$$

i.e,

$$\frac{\tau_M}{L} \cong \left(\frac{t}{4k_z^2\sigma^2}\right)^{\frac{1}{n}}. \quad (18)$$

We obtain that, for very rough surfaces, $\tau_M \ll L$, i.e. the correlation length of the returns is much smaller than the correlation length of the surface heights.

Conversely, expression (16) is meaningless if

$$k_z\sigma < \frac{\sqrt{t}}{2}. \quad (19)$$

This is related to the fact that the minimum value of the correlation in (13) is the product of statistical means, i.e., $\exp(-4k_z^2\sigma^2)$, which is negligible for $4k_z^2\sigma^2 \gg 1$. If σ is small, this minimum value is no longer negligible, and this should be accounted for by setting a σ-dependent threshold for the correlation in (13). However, this complication can be avoided by noting that the correlation length of the returns cannot exceed the correlation length of surface roughness - in fact, the lack of correlation of surface heights (and hence their independence, since they are Gaussian) implies the independence of their exponentials in (13) - and that for values of $k_z\sigma$ just below unity τ_M is of the order of *L*. Accordingly, it is reasonable to use (16) whenever surface roughness is such that (16) leads to $\tau_M/L<1$, and to set $\tau_M/L=1$ otherwise.

Now we can also evaluate the equivalent number of scatterers per resolution cell as the ratio between the cell area *A* and $\pi\tau_M^2$:

$$N = \frac{A/\pi L^2}{\left[-\ln\left(1-\frac{t}{4k_z^2\sigma^2}\right)\right]^{\frac{2}{n}}} = N\left(\frac{A}{\pi L^2}, k_z\sigma, n\right). \quad (20)$$

From (20) it is evident that the number of equivalent scatterers per resolution cell is a function of:

- the resolution cell area A normalized to the area of a circle with radius equal to the correlation length of the surface L;

- the relative surface roughness $k_z\sigma$;

- the shape of the autocorrelation function.

In Fig. 2 the behavior of N as a function of $A/\pi L^2$ is shown, fixing the shape of the autocorrelation function (a) and the relative surface roughness (b). As expected, the number of scatterers increases linearly with the increase of $A/\pi L^2$. Note that from now on the value of the correlation threshold is fixed to 1. All the presented graphs are plotted only for values of the number of equivalent scatterers per resolution cell N lower than 10: in this way, only the range for which a significant departure from the Exponential model is experienced is investigated.

In Fig. 3 N is shown as a function of $k_z\sigma$, fixing $A/\pi L^2$ (a) and the shape of the autocorrelation function (b). As expected, the number of scatterers increases with the increase of the surface roughness. In particular, the influence of the chosen autocorrelation function is relevant: this unveils one of the weak points in the use of classical surface models, for which no straightforward procedure for the identification of the true autocorrelation function exists. Conversely, as shown in the previous section the use of the fractal fBm model requires no arbitrary choice for the autocorrelation, because its shape is automatically fixed by the surface model itself. Note that no graph of the behavior of N as a function of n is provided because the case of intermediate n values is of small practical interest in the context of this paper.

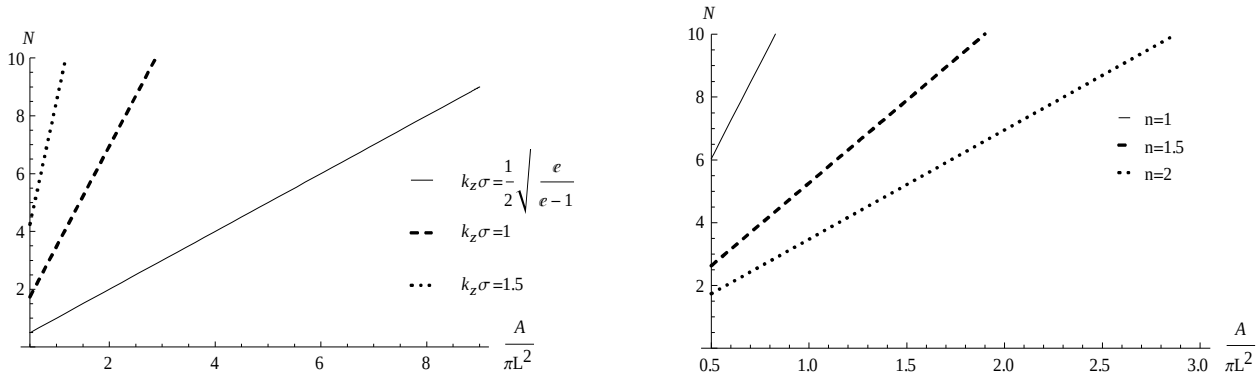

(a) (b)

Fig. 2: Number of scatterers per resolution cell plotted as a function of $A/\pi L^2$. In (a) the Gaussian autocorrelation function of (4) is assumed, while in (b) $k_z\sigma$=1 and the autocorrelation function of (6) is assumed with the values of n provided in the legend.

In Fig. 4 we provide the plot of the number of scatterers N as a function of the correlation length of the surface L for three different values of σ and for a Gaussian auto-correlation function. The parameters reported in Table I, corresponding to the Cosmo-SkyMed Enhanced Spotligth SAR sensor are used in the evaluation of $k_z = (2\pi/\lambda)\cos(\vartheta)$ in (14) and of the number of

independent scatterers *N*. Typical values of the roughness parameters are considered [14], [20], [22]. A wider discussion regarding the typical values of the roughness parameters of natural surfaces is reported in the Appendix. It can be noted from the graphs that in many actual situations the number of equivalent scatterers per resolution cell is far below 10. In these cases the speckle is partially developed.

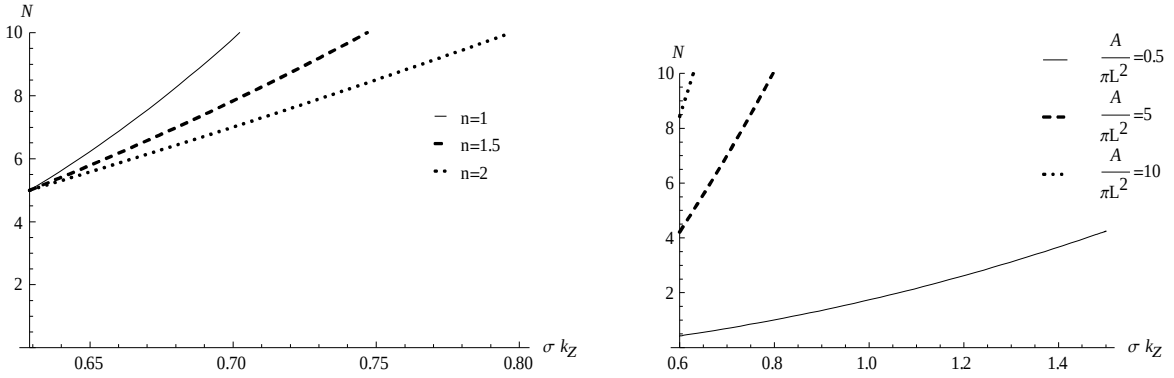

Fig. 3: Number of scatterers per resolution cell plotted as a function of $k_z\sigma$. In (a) $A/\pi L^2$=5 and the autocorrelation function of (6) is assumed with the values of *n* provided in the legend; in (b) the Gaussian autocorrelation function of (4) is assumed.

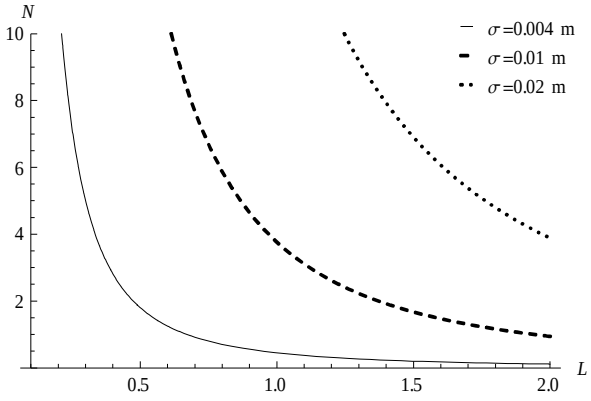

Fig. 4: Plot of the number of scatterers *N* as a function of the correlation length of the surface *L* [m] assuming the (Cosmo-SkyMed) parameters reported in Table I.

B. Fractal surface model

If a fractal model is assumed for the surface, the structure function (10) can be used into (14), thus obtaining, along guidelines similar to those provided in the above sub-section, the following size for the equivalent scatterers:

$$\tau_M = \left(\frac{\sqrt{t}}{\sqrt{2}k_z T^{1-H}}\right)^{\frac{1}{H}}. \qquad (21)$$

Note that (21) can be used for any value of the surface roughness fractal parameters, because the minimum value of the correlation in (13) is zero. This is related to the infinite-variance property of fBm [8]-[11].

Also in this case we can evaluate the equivalent number of scatterers per resolution cell as the ratio between the cell area and $\pi\tau_M^2$, obtaining:

$$N = \frac{A}{\pi\left(\frac{\sqrt{t}}{\sqrt{2}k_z T^{1-H}}\right)^{\frac{2}{H}}} = \frac{Ak_z^2}{\pi\left(\frac{\sqrt{t}}{\sqrt{2}(k_z T)^{1-H}}\right)^{\frac{2}{H}}} = N(Ak_z^2, k_z T, H). \qquad (22)$$

From (22) we can assess that the number of equivalent scatterers per resolution cell is a function of:

- the relative resolution cell area Ak_z^2;

- the relative surface roughness $k_z T$;

- the Hurst parameter H.

Also in this case some plots of N as a function of its parameters are reported. These plots illustrate behaviors of N that cannot be intuitively anticipated without considering in detail the relation between fractal parameters and surface roughness. In Fig. 5, N is shown as a function of Ak_z^2, assuming to fix H (a) and $k_z T$ (b). In this case, as expected, the number of scatterers increases linearly with the increase of Ak_z^2. Note that, as in the previous case, the value of the correlation threshold t is fixed to 1 and all the presented graphs are plotted only in the range where the number of equivalent scatterers per resolution cell is not larger than 10.

In Fig. 6 the behavior of N as a function of $k_z T$ is shown, assuming to fix Ak_z^2 (a) and H (b). The number of scatterers increases with the increase of the relative surface roughness. No graph of N as a function of H is provided because, due to the limited range of the considered values of H ($H \in [0.6, 0.8]$), we think that this behavior is adequately illustrated by the graphs presented in Fig. 5 (b) and 6 (a).

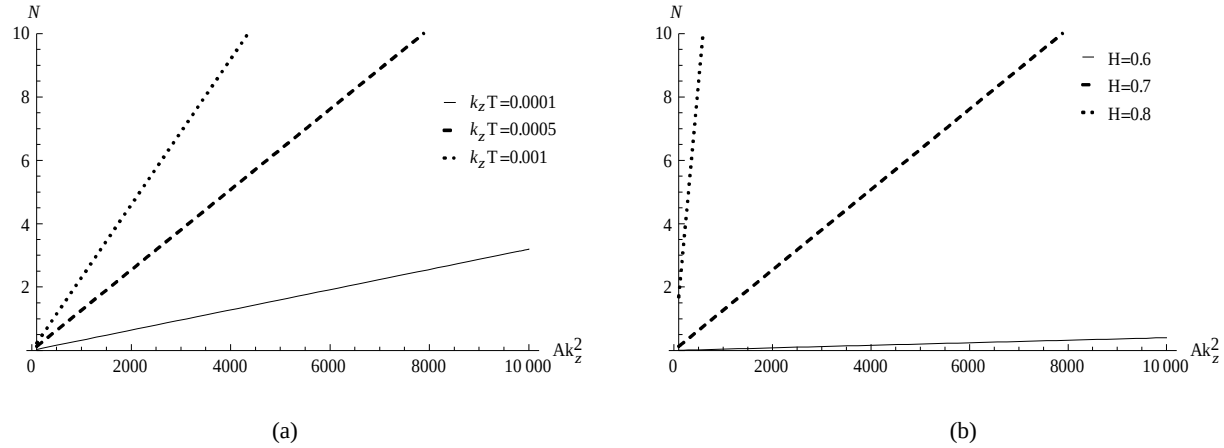

(a) (b)

Fig. 5: Number of scatterers per resolution cell plotted as a function of Ak_z^2. In (a) H=0.7, while in (b) $k_z T$=0.0005.

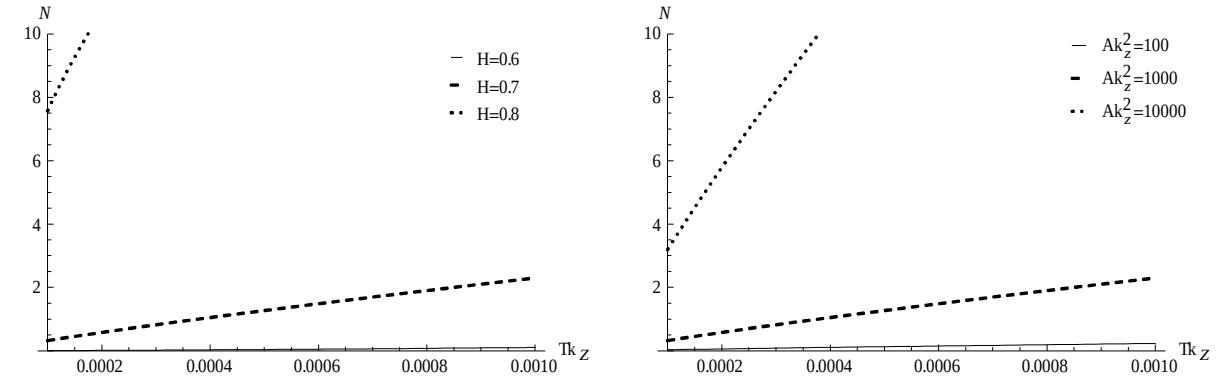

(a) (b)

Fig. 6: Number of scatterers per resolution cell plotted as a function of $k_z T$. In (a) Ak_z^2=1000, while in (b) H=0.7.

Finally, in Fig. 7 we provide the plot of the number of scatterers N as a function of the topothesy T of the surface - again for the usual three values of H – for the Cosmo-SkyMed SAR sensor whose parameters are reported in Table I. The used fractal parameters are in accordance with typical values for natural surfaces reported in the open literature [13], [14], [16], [23], [26]. A wider discussion on typical values of the fractal parameters of natural surfaces is reported in the Appendix. Figure 7 clearly shows that for resolution cell dimensions typical of high resolution SAR sensors, and for typical values of the fractal parameters of a natural surface, the number of scatterers per resolution cell can approach unity in many practical cases. When this is the case, the speckle cannot be treated as fully developed and the K-distribution introduced in (2) should be used, after substitution of the appropriate number of equivalent scatterers N, which - if the fractal parameters of the observed surface are known or can be retrieved directly from SAR data [27], [28] - can be evaluated using (22).

TABLE II
REALIZATIONS OF THE RESOLUTION CELL ROUGHNESS

	$T=10^{-6}$ m	$T=4*10^{-6}$ m
$H=0.6$	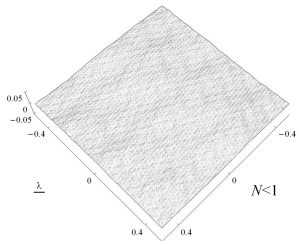 $N<1$	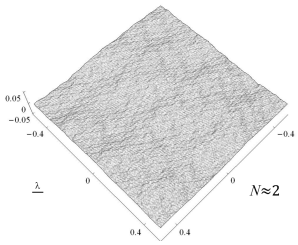 $N\approx 2$
$H=0.7$	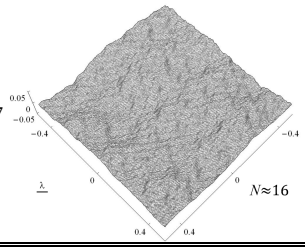 $N\approx 16$	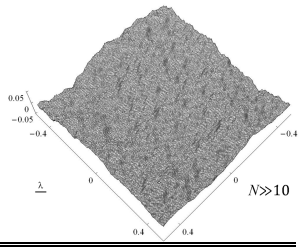 $N\gg 10$

Examples of realizations of the surface roughness within the resolution cell for different fractal parameters are presented: for each realization the approximate number of equivalent scatterers is reported. The sensor parameters reported in Table I are used.

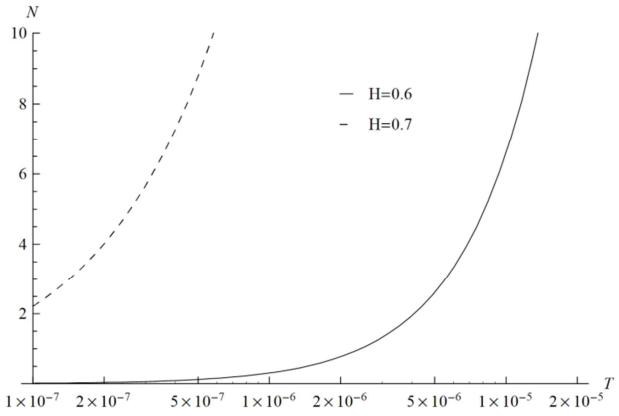

Fig. 7: Plot of the number of scatterers N as a function of the topothesy of the surface T [m] assuming the (Cosmo-SkyMed) parameters reported in Table I (T-axis is in logarithmic scale). Note that in this case the values for H=0.8 are out of the represented range for N.

In Table II four examples of realizations of the surface roughness within the resolution cell are presented: these figures provide a visual reference for the considered fractal roughness. The surface is synthesized using the Weierstrass-Mandelbrot fractal function, which effectively approximates the behavior of an fBm surface [9]. Looking at the figures, the relation between the effective number of scatterers and the roughness of the surface at spatial scales of the order of the resolution cell size can be appreciated.

V. CONCLUSIONS

In this paper a physical model for the assessment of speckle statistics in SAR images of natural soil surfaces was presented. The mathematical formalism previously introduced in the scientific literature for the description of partially developed speckle was used. Accordingly, the image distribution was parameterized in terms of the number of independent scatterers per resolution cell.

A rationale for determining the equivalent scatterer sizes was introduced, allowing to analytically evaluate the equivalent number of scatterers per resolution cell as a function of physical observables: surface roughness and sensor parameters. The presented model can be applied to both classical and fractal surface roughness descriptions. Use of the latter for natural surfaces has been here shown to be preferable to study also the speckle phenomenon. As a matter of fact, in the fractal case the equivalent number of scatterers depends on two surface parameters only, the Hurst coefficient and topothesy, whereas in the classical case the surface standard deviation and correlation length must be supported by the surface autocorrelation shape, that even for single-scale surfaces implies dealing with at least one more parameter.

We have shown that, when the area of the resolution cell typical of modern space-borne SAR (e.g., Cosmo-SkyMed, TerraSAR-X, with particular focus on the spotlight operational mode) is considered, the equivalent number of scatterers can be not very large and of the order of unity in many practical cases for not very smooth surfaces, presenting typical values of natural surface roughness. In these cases the hypothesis of fully developed speckle fails and the K-distributed model can be applied.

The availability of a closed form expression for the evaluation of the equivalent number of scatterers per resolution cell N allows the development of direct models which can be used for simulation purposes. In this paper, we generated surface roughness for resolution cells whose equivalent number of scatterers (to be determined after the sensor parameters have been postulated) can be easily evaluated, see Table II. Available simulation techniques [29] allow generating (for instance via Monte Carlo approaches) the corresponding SAR images for an homogeneous area; this step is supported by the knowledge, in analytical form, of the Cumulative Distribution Function relevant to K-distributed random variables [4]. Visual comparison with actual SAR images for homogeneous areas may lead to infer about sub-resolution properties of the surface (e.g., fractal parameters). This inversion step could be also performed at a more rigorous level by estimating, directly from the SAR images, the K-distribution parameters [30], that, by means of the model presented in this paper, can be linked to fractal surface parameters, i.e., to sub-resolution physical surface quantities. We think this is the main future development expected after this paper.

APPENDIX

TYPICAL ROUGHNESS PARAMETERS OF NATURAL SURFACES

In order to better highlight the relevance of the presented results, the knowledge of typical values of the roughness of natural surfaces is necessary. In this appendix we present a review of typical measured values of the roughness parameters of natural surfaces for both classical and fractal surface models.

With regard to classical models, it is necessary to stress that the stationary behavior advocated in order to use these models is at best a limiting behavior among natural surfaces [8], [14]-[17], [24]. As a matter of fact, in the great majority of cases the measured values of the rms height and correlation length show a dependence on the size of the considered profile [8]-[11], [13]-[17]. This kind of behavior is related to the non-stationary fractal characteristics of the examined natural profiles. For band-limited fractal surfaces some authors introduce equivalent rms heights and correlation lengths, and provide expressions describing them as functions of the profile length [9], [13]-[15]. However, even when the assumption of a stationary model can be considered reasonable, stringent conditions must be enforced for the precise measurement of the roughness parameters. In particular, to attain accurate estimates of both rms height and correlation length, the profile size must be very large with respect to the true correlation length (at least 200 times larger) [14], [21]. Given all these limitations, not many reliable measurements of classical surface roughness parameters are available in the literature. An accurate list of parameters can be found in [14], where a critical review of the data available at the time of publication is presented. The reported values of the rms height range from a minimum of 0.0007 m to a maximum of 0.269 m, while those relevant to the correlation length range from 0.022 m to 6.50 m. It is worth noting that the evaluation of the correlation length requires a preliminary fitting of measured data in order to obtain the shape of the autocorrelation function, which is necessary for the evaluation of the correlation length [14]. Other valuable measurements are available in the literature and are in accordance with the values reported above, confirming that natural bare soil is usually well described with an rms height of the order of centimeters or fraction of centimeter and a correlation length of the order of tens of centimeters [19], [20], [22].

TABLE III
TYPICAL VALUES OF THE FRACTAL PARAMETERS OF NATURAL SURFACES

Surface Type	H	T [m]
Playa	0.67	$6.94 \cdot 10^{-5}$
Cobbles	0.73	$1.07 \cdot 10^{-6}$
Pahoehoe	0.78	$2.35 \cdot 10^{-5}$
Lava flows	[0.49, 0.73]	$[7.64 \cdot 10^{-5}, 0.13]$
Debris flow 1	0.67	$3.22 \cdot 10^{-3}$
Debris flow 2	0.65	$5.27 \cdot 10^{-3}$
Sedimented plain	0.75	$2.61 \cdot 10^{-3}$
Alluvial fans	[0.64, 0.85]	$[8.35 \cdot 10^{-6}, 5.76 \cdot 10^{-3}]$
Siltstone rocks	0.63	$\sim 7.36 \cdot 10^{-8}$

With regard to the fractal models, the main problem in referring typical values of fractal dimension and topothesy is the heterogeneity of provided parameters encountered among different publications. For instance, in [13] the values of the rms height and rms slope at different scales are provided, along with the Hurst parameter, for a wide set of surfaces of interest in geological studies. Thanks to this information, the values of the topothesy of the surfaces can be computed [9]. However, fractal surfaces are frequently described using spectral parameters: this is due to the fact that fractal processes present the remarkable property of holding power law spectra, expressed as

$$S(k) = S_0 k^{-\alpha}, \tag{23}$$

wherein S_0 is the power spectrum offset, k is the wavenumber, and α the spectral exponent. For a one-dimensional profile (in fact, measurements are usually performed on one-dimensional profiles, assuming isotropy for the observed surfaces) α is related to the Hurst parameter H and S_0 to the topothesy T via the following expressions [9]:

$$\alpha = 1 + 2H \tag{24}$$

$$S_0 = T^{2-2H} \frac{\pi H}{\cos(\pi H)} \frac{1}{\Gamma(1-2H)}, \tag{25}$$

$\Gamma(\cdot)$ being the Euler Gamma function. Inverting (24) and (25) it is possible to compute the fractal parameters H and T from α and S_0. Further care should be taken to the fact that in many references the spectral parameters are provided in the spatial frequency f domain and not in the wavenumber one, which is the domain of reference of (23)-(25). In this case, taking into account that $k = 2\pi f$, the relation between S_0 and the spectral offset c evaluated in the spatial frequency domain is

$$S_0 = c \cdot (2\pi)^{\alpha}. \qquad (26)$$

Considering these observations, typical values of the fractal parameters can be obtained from [14]. To provide a more readable list of the parameters of interest, in Table III we report the values presented in [14] converted in terms of *H* and *T*. In a couple of cases ranges are reported, rather than exact values. In the last row of Table III we also include the values retrieved from [16], where the spectral offset *c* was graphically obtained by using the plots of the spectra and, for this reason, the value of *T* is reported as an approximate one. Looking at the values reported in the table, we can conclude that for natural surfaces the typical values of *H* are in the range [0.6, 0.8] and those of *T* in [10^{-7} m, 10^{-3} m].

REFERENCES

[1] P. Beckman and A. Spizzichino, *The Scattering of Electromagnetic Waves from Rough Surfaces*. New York: Pergamon Press, 1963.

[2] F. T. Ulaby, R. K. Moore, and A. K. Fung, *Microwave Remote Sensing, Active and Passive*. Norwood, MA: Artech House, 1986.

[3] J. W. Goodman, "Some fundamental properties of speckle", *J. Opt. Soc. Am.*, vol. 66, no. 11, pp. 806-814, Nov. 1976.

[4] E. Jakeman and P. N. Pusey, "A Model for Non-Rayleigh Sea Echo", *IEEE Trans. Antennas Propag.*, vol. 24, no. 6, pp. 1145-1150, Nov. 1976.

[5] C. J. Olivier, "A model for non-Rayleigh scattering statistics", *Opt. Acta*, vol. 31, no. 6, pp. 701-722, 1984.

[6] J. K. Jao, "Amplitude distribution of composite terrain radar clutter and the K-distribution", *IEEE Trans. Antennas Propag.*, vol. 32, no. 10, pp. 1049-1062, Oct. 1984.

[7] K. Ouchi, S. Tajbakhsh, and R. E. Burge, "Dependence of Speckle Statistics on Backscatter Cross-Section Fluctuations in Synthetic Aperture Radar Images of Rough Surfaces," *IEEE Trans. Geosci. Remote Sens.*, vol. GE-25, no. 5, pp. 623–628, Sep. 1987.

[8] B. B. Mandelbrot, *The Fractal Geometry of Nature*. New York: Freeman, 1983.

[9] G. Franceschetti and D. Riccio, *Scattering, Natural Surfaces and Fractals*. Burlington, MA: Academic Press, 2007.

[10] J. S. Feder, *Fractals*. New York: Plenum, 1988.

[11] K. Falconer, *Fractal Geometry*. Chichester, U.K.: Wiley, 1989.

[12] L. Tsang and J.A. Kong, *Scattering of Electromagnetic Waves, Vol. 3: Advanced Topics*. Wiley Interscience, 2001.

[13] M. K. Shepard, B. A. Campbell, M. H. Bulmer, T. G. Farr, L. R. Gaddis, and J. J. Plaut, "The roughness of natural terrain: A planetary and remote sensing perspective", *J. Geophys. Res.*, vol. 106, no. E12, pp. 32 777–32 795, Dec. 2001.

[14] W. Dierking, "Quantitative Roughness Characterization of Geological Surfaces and Implications for Radar Signature Analysis," *IEEE Trans. Geosci. Remote Sens.*, vol. 37, no. 5, pp. 2397–2412, Sep. 1999.

[15] B. A. Campbell, "Scale-dependent surface roughness behavior and its impact on empirical models for radar backscatter", *IEEE Trans. Geosci. Remote Sens.*, vol. 47, no. 10, pp. 3480-3488, Oct. 2009.

[16] S. R. Brown and C. H. Scholz, "Broad-band study of the topography of natural rock surfaces," *J. Geophys. Res.*, vol. 90, no. B14, pp. 12 575–12 582, Dec. 1985.

[17] D. L. Turcotte, *Fractals and Chaos in Geology and Geophysics*. Cambridge University Press, 1997.

[18] J. Shi, J. Wang, A. Y. Hsu, P. E. O. Neill, and E. T. Engman, “Estimation of Bare Surface Soil Moisture and Surface Roughness Parameter Using L-band SAR Image Data,” *IEEE Trans. Geosci. Remote Sens.*, vol. 35, no. 5, pp. 1254–1266, Sep. 1997.

[19] Q. Li, J. Shi, and K. S. Chen, “A Generalized Power Law Spectrum and its Applications to the Backscattering of Soil Surfaces Based on the Integral Equation Model,” *IEEE Trans. Geosci. Remote Sens.*, vol. 40, no. 2, pp. 271–280, Feb. 2002.

[20] Y. Oh, K. Sarabandi, and F. T. Ulaby, “An Empirical Model and an Inversion Technique for Radar Scattering from Bare Soil Surfaces,” *IEEE Trans. Geosci. Remote Sens.*, vol. 30, no. 2, pp. 370–381, March 1992.

[21] Y. Oh and Y. C. Kay, “Condition for Precise Measurement of Soil Surface Roughness,” *IEEE Trans. Geosci. Remote Sens.*, vol. 36, no. 2, pp. 691–695, March 1998.

[22] M. Zribi, V. Ciarletti, O. Taconet, J. Paille, and P. Boissard, “Characterisation of the Soil Structure and Microwave Backscattering Based on Numerical Three-Dimensional Surface Representation: Analysis with a Fractional Brownian Model,” *Remote Sens. Environ.*, vol. 72, pp. 159–169, 2000.

[23] G. Franceschetti, A. Iodice, M. Migliaccio, D. Riccio, "Scattering from natural rough surfaces modeled through fractal Brownian motion two-dimensional processes", *IEEE Trans. Geosci. Remote Sens.*, vol. 47, no. 9, pp. 1405-1415, Sep. 1999.

[24] R. S. Sayles and T. R. Thomas, “Surface topography as a nonstationary random process,” *Nature*, vol. 271, pp. 431–434, 1978.

[25] G. Franceschetti and G. Schirinzi, “A SAR processor based on two-dimensional FFT codes,” *IEEE Trans. Aerosp. Electron. Syst.*, vol. 26, no. 2, pp. 356–366, March 1990.

[26] T. Austin, A. W. England, G. H. Wakefield, “Special problems in the estimation of power-law spectra as applied to topographical modeling”, *IEEE Trans. Geosci. Remote Sens.*, vol. 32, no. 4, pp. 928-939, July 1994.

[27] G. Di Martino, A. Iodice, D. Riccio and G. Ruello, “Imaging of Fractal Profiles”, *IEEE Trans. Geosci. Remote Sens.*, vol. 48, no. 8, pp. 3280-3289, Aug. 2010.

[28] G. Di Martino, D. Riccio and I. Zinno, "SAR Imaging of Fractal Surfaces", *IEEE Trans. Geosci. Remote Sens.*, vol. 50, no. 2, pp. 630-644, Feb. 2012.

[29] A. Papoulis, *Probability, Random Variables, and Stochastic Processes*, Singapore: McGraw-Hill, 1984.

[30] I. R. Joughin, D. B. Percival, and D. P. Winebrenner, "Maximum likelihood estimation of K distribution parameters for SAR data," *IEEE Trans. Geosci. Remote Sens.*, vol.31, no.5, pp.989-999, Sep. 1993.